Full time-dependent Hartree-Fock solution of large N Gross-Neveu models

Gerald V. Dunne[1,2] and Michael Thies[3]

[1]*ARC Centre of Excellence in Particle Physics at the Terascale and CSSM, School of Chemistry and Physics, University of Adelaide, Adelaide, South Australia 5005, Australia*

[2]*Physics Department, University of Connecticut, Storrs, Connecticut 06269, USA*

[3]*Institut für Theoretische Physik, Universität Erlangen-Nürnberg, D-91058 Erlangen, Germany*

(Received 17 September 2013; published 13 January 2014)

We find the general solution to the time-dependent Hartree-Fock problem for scattering solutions of the Gross–Neveu models, with both discrete (GN_2) and continuous (NJL_2) chiral symmetry. We find new multibreather solutions both for the GN_2 model, generalizing the Dashen–Hasslacher–Neveu breather solution, and also new twisted breathers for the NJL_2 model. These solutions satisfy the full time-dependent Hartree-Fock consistency conditions, and only in the special cases of GN_2 kink scattering do these conditions reduce to the integrable Sinh–Gordon equation. We also show that all baryons and breathers are composed of constituent twisted kinks of the NJL_2 model. Our solution depends crucially on a general class of transparent, time-dependent Dirac potentials found recently by algebraic methods.

DOI: 10.1103/PhysRevD.89.025008 PACS numbers: 11.10.Kk, 11.27.+d, 11.10.-z

I. INTRODUCTION

The Gross–Neveu (GN_2) and Nambu–Jona-Lasinio (NJL_2) models in $1+1$-dimensional quantum field theory describe N species of massless, self-interacting Dirac fermions with Lagrangians [1]:

$$\mathcal{L}_{\rm GN} = \sum_{k=1}^{N} \bar\psi_k i\partial\!\!\!/ \psi_k + \frac{g^2}{2}\left(\sum_{k=1}^{N}\bar\psi_k\psi_k\right)^2 \tag{1.1}$$

$$\mathcal{L}_{\rm NJL} = \sum_{k=1}^{N} \bar\psi_k i\partial\!\!\!/ \psi_k + \frac{g^2}{2}\left[\left(\sum_{k=1}^{N}\bar\psi_k\psi_k\right)^2 + \left(\sum_{k=1}^{N}\bar\psi_k i\gamma_5\psi_k\right)^2\right]. \tag{1.2}$$

These models serve as soluble paradigms for symmetry breaking phenomena in both strong interaction particle physics and condensed matter physics [2,3]. We consider these models in the 't Hooft limit, $N\to\infty$, with $Ng^2 =$ constant, where semiclassical methods become exact. Classically, the GN_2 model has a discrete chiral symmetry, while the NJL_2 model has a continuous chiral symmetry. At finite temperature and density, these models exhibit a rich structure of phases with inhomogeneous crystalline condensates in the large N limit, these phases being directly associated with chiral symmetry breaking [4]. Such self-interacting fermion models also have numerous applications to a wide variety of phenomena in particle, condensed matter, and atomic physics [5–21].

In the 't Hooft limit, $N\to\infty$, $Ng^2 =$ constant, we use semiclassical techniques pioneered in this context by Dashen, Hasslacher, and Neveu (DHN) [22]. This can either be understood in functional language as a gap equation, or as a Hartree-Fock (HF) problem in which one solves the Dirac equation subject to constraints on the scalar and pseudoscalar condensates. Here we use the time-dependent Hartree-Fock (TDHF) formalism, which involves solving the following constrained Dirac equations:

$$GN_2:\ (i\partial\!\!\!/ - S(x,t))\psi_\alpha = 0, \quad S = -g^2\sum_{\beta}^{\rm occ}\bar\psi_\beta\psi_\beta \tag{1.3}$$

$$NJL_2:\ (i\partial\!\!\!/ - S(x,t) - i\gamma_5 P(x,t))\psi_\alpha = 0,$$
$$S = -g^2\sum_{\beta}^{\rm occ}\bar\psi_\beta\psi_\beta, \qquad P = -g^2\sum_{\beta}^{\rm occ}\bar\psi_\beta i\gamma_5\psi_\beta. \tag{1.4}$$

For NJL_2 it is convenient to combine the scalar and pseudoscalar condensates into a single complex condensate:

$$\Delta = S - iP. \tag{1.5}$$

All *static* solutions to these HF problems have been found and used to solve analytically the equilibrium thermodynamic phase diagrams of these models in the large N limit, at finite temperature and nonzero baryon density [3,4]. These static solutions reveal a deep connection to integrable models, in particular the modified Korteweg-de Vries system for the GN_2 system and Ablowitz-Kaup-Newell-Segur for the NJL_2 system [4,23]. In this paper we present a significant extension of these results, by finding the full set of time-dependent solutions to the TDHF equations in Eqs. (1.3) and (1.4) [24]. We solve these problems in generality, describing the time-dependent scattering of nontrivial topological objects such as kinks, baryons, and

breathers. Some special cases have been solved previously, but here we present several entirely new classes of solutions to the TDHF problem. Surprisingly, we have found that the most efficient strategy is to solve the (apparently more complicated) NJL_2 model first and then obtain GN_2 solutions by imposing further constraints on these solutions. For example, we show that the GN_2 baryons found by Dashen, Hasslacher, and Neveu [22] can be thought of as bound objects of twisted NJL_2 kinks and furthermore that the scattering of the GN_2 baryons can be deduced from the scattering of twisted kinks, a problem the solution of which we present here. Breathers are somewhat more involved, but again we give a complete and constructive derivation of all multibreather solutions, also in terms of constituent twisted kinks. This includes new breather and multibreather solutions in NJL_2 as well as new multibreather solutions in the GN_2 model.

We stress that, while it is well known that the classical equations of motion for the GN_2 and NJL_2 models are closely related to integrable models [25–27], this fact is only directly useful for the solution of the time-dependent Hartree-Fock problem for the simplest case of kink scattering in the GN_2 model, where the problem reduces to solving the integrable nonlinear Sinh–Gordon equation [28–30]. The more general self-consistent TDHF solutions that we find here *do not* satisfy the Sinh–Gordon equation or any simple general bosonic nonlinear equation. Instead we shall make use of the transparent, time-dependent Dirac potentials derived recently by solving a finite algebraic problem [31]. We also emphasize that these more general solutions require a self-consistency condition relating the filling fraction of valence fermion states to the parameters of the condensate solution, as for the static GN_2 baryon [22], the static twisted kink [32], and the GN_2 breather [22]. For our time-dependent solutions, this important fact means that during scattering processes there is nontrivial backreaction between fermions and their associated condensates and densities [33]. Kink scattering in the GN_2 model, described by Sinh–Gordon solitons [28–30], is much simpler because there is no fermion filling-fraction self-consistency condition, nor backreaction.

A. Basic building blocks

The known Hartree-Fock solutions are characterized by several basic building blocks: kinks, baryons, and breathers. We briefly review these solutions below. In fact we show in this paper that the general solutions are all built out of one basic unit, the twisted kink. To simplify the notation, we henceforth set $m = 1$, measuring dimensional quantities in terms of the dynamically generated fermion mass m.

1. Real CCGZ kink for GN_2

The most familiar HF solution for the GN_2 model is the static Coleman–Callan–Gross–Zee (CCGZ) kink [22]. Since we can restrict ourselves to potentials which go to 1 for $x \to -\infty$ without loss of generality, we quote the "antikink":

$$\text{condensate}: S(x) = -\tanh x = \frac{1-e^{2x}}{1+e^{2x}}$$
$$\text{fermion filling-fraction consistency condition}: \text{none}. \quad (1.6)$$

We have expressed the usual tanh form as a ratio of polynomials of exponentials, as this is the basic form of the more general solutions. The fermion number is $N(\nu - 1/2)$, where $\nu \in [0, 1]$, the filling fraction of the zero energy bound state, is not constrained by the self-consistency requirement for the scalar condensate $\langle\bar{\psi}\psi\rangle$. This static kink can be boosted with some velocity to produce a simple time-dependent solution.

2. Complex twisted kink for NJL_2

The corresponding kinklike solution for the NJL_2 model, Shei's twisted kink [32], can be expressed in terms of the complex condensate Δ defined in Eq. (1.5):

$$\text{condensate}: \Delta(x) = \frac{1+e^{-2i\theta}e^{2x\sin\theta}}{1+e^{2x\sin\theta}}$$
$$\text{fermion filling-fraction consistency condition}: \nu = \frac{\theta}{\pi}. \quad (1.7)$$

For $\theta > 0$ this kink rotates through an angle -2θ in the chiral (S, P) plane as x goes from $-\infty$ to $+\infty$. Notice that both the magnitude, $|\Delta(x)|$, and the phase, $\arg\Delta(x)$, vary with x. When $\theta = \pi/2$, the twisted kink becomes real and reduces to the GN_2 kink in Eq. (1.6). As in Eq. (1.6), the solution can be expressed as a rational function of simple exponentials. This twisted kink solution reveals a new level of complexity, as the self-consistency of the HF solution requires a relation between the chiral angle parameter θ and the fermion filling fraction of the valence bound state [32]. This fact is responsible for more intricate scattering dynamics of twisted kinks, as there is a backreaction from the bound fermions during scattering processes, a phenomenon that does not occur for scattering of CCGZ kinks in the GN_2 model. The difference between the twisted kink and the CCGZ kink is due to the fact that there is no self-consistency condition for the pseudoscalar condensate $\langle\bar{\psi}i\gamma_5\psi\rangle$ in the GN_2 model. This is discussed in detail below. Note that the single twisted kink in Eq. (1.7) can also be boosted with some velocity to produce a simple time-dependent solution.

3. Real DHN baryon for GN_2

DHN found a self-consistent static baryon solution for the GN_2 model that looks like a bound kink and antikink, at locations $x = \pm c_0/y$ [22]:

$$\text{condensate: } S(x) = 1 + y[\tanh(yx - c_0) - \tanh(yx + c_0)] = \frac{1 + \frac{2\cos 2\theta}{\cos\theta} e^{2yx} + e^{4yx}}{1 + \frac{2}{\cos\theta} e^{2yx} + e^{4yx}}, \qquad y = \sin\theta,$$
$$c_0 = \frac{1}{2}\, ar\tanh\, y, \text{ fermion filling-fraction consistency condition: } \nu_+ - \nu_- = \frac{2\theta}{\pi} - 1. \tag{1.8}$$

The filling fractions ν_+, ν_- refer to the positive and negative energy bound states, respectively. As $y \to 1$, one or the other of the kink or antikink decouples, leaving a single CCGZ kink or antikink. For this solution, self-consistency requires a relation between the parameter y and the fermion filling fractions of the valence bound states [22]. This means that the physical size ($\sim c_0$) of the baryon is directly related to the number of valence fermions that it binds and results in intricate fermion dynamics during the scattering of DHN baryons [33]. This static baryon solution can also be boosted to a given velocity. In this paper we present the apparently new result that the DHN baryon can be expressed as a bound pair of twisted kinks, where the twist parameters are directly related to the baryon parameter y; see below, Sec. III B.

4. Real DHN breather for $\mathbf{GN_2}$

DHN also found in the GN_2 model an exact time-dependent self-consistent HF solution that is periodic in time in its rest frame (known as the "breather") [22]:

$$\text{condensate: } S(x,t) = \frac{1 + b(2-K^2)e^{Kx} - 2ae^{Kx}\cos(\Omega t) + e^{2Kx}}{1 + 2be^{Kx} + 2ae^{Kx}\cos(\Omega t) + e^{2Kx}}$$
$$\Omega = \frac{2}{\sqrt{1+\epsilon^2}}, \qquad K = \epsilon\Omega, \qquad a = \frac{\epsilon}{2}\sqrt{4b^2 - 4 - K^2 b^2} \tag{1.9}$$
$$\text{filling-fraction consistency condition: } b = (\nu_- - \nu_+)\frac{\sqrt{1+\epsilon^2}}{1 - (2/\pi)\arctan\,\epsilon}.$$

The DHN breather has two parameters, ϵ and b, characterizing the frequency and the amplitude of its oscillation. The breather also requires a self-consistency relation between the valence fermion filling fractions and the breather parameters [22,34].

B. Building multiple-object solutions

The aforementioned exact solutions have been generalized in various ways. First, as mentioned already, it is clear that each can be boosted from its rest frame. What is less clear is that they can be boosted independently, to describe scattering processes of independent objects. We show in this paper how this can be done in a fully self-consistent manner:

1. The real CCGZ kinks for GN_2 can be combined into static multikink solutions [35] and also kink-antikink crystals [3]. Exact solutions can also be given describing the scattering of arbitrary combinations of kinks and antikinks, with arbitrary velocities. This construction is based on the fact that the logarithm of the scalar condensate S satisfies the Sinh–Gordon (ShG) equation [28,29], so these solutions can be constructed from the corresponding ShG solitons [30]. No fermion filling-fraction self-consistency condition is required.
2. Takahashi *et al*. [36] have recently presented an algebraic construction for static multi-twisted-kink solutions for the NJL_2 model, and twisted crystalline solutions were constructed in Ref. [37]. In the present paper, we give new results for the *time-dependent* scattering of arbitrary combinations of twisted kinks, with arbitrary velocities. Note that the twisted kinks do not satisfy the Sinh–Gordon equation, so the construction uses other methods. We find a simple closed-form solution as a ratio of determinants, for both the static and time-dependent multi-twisted-kink solutions.
3. The scattering of two DHN baryons for the GN_2 model was solved in Ref. [33], and an algorithmic procedure for the description of multi-DHN-baryon scattering was presented in Ref. [38]. In this paper we show that DHN baryons can be constructed as bound twisted kinks, and therefore the scattering of DHN baryons can be described as special cases of the scattering of twisted kinks, for which we have a closed-form solution.
4. Our construction leads to two new results concerning breathers. First, we find twisted breather solutions for the NJL_2 model, and we find solutions describing the scattering of any number of these twisted breathers. Second, as a consequence, we find the general solution for the scattering of any number of GN_2 breathers. This is consistent with the partial results of Ref. [34]. Indeed, our general construction describes the scattering of any number of any of these objects: real kinks, twisted kinks, DHN GN_2 baryons and breathers, and NJL_2 breathers.

C. Dirac equation and kinematic notation

We consider the TDHF problem (1.4) for the NJL_2 model, and later we specialize to solutions of the GN_2

model. We work with the following representation of the Dirac matrices:

$$\gamma^0 = \sigma_1, \qquad \gamma^1 = i\sigma_2, \qquad \gamma_5 = \gamma^0\gamma^1 = -\sigma_3, \quad (1.10)$$

and it is convenient to adopt light-cone coordinates (note that $\bar{z}$ is not the complex conjugate of z),

$$z = x - t, \quad \bar{z} = x + t, \quad \partial_0 = \bar{\partial} - \partial, \quad \partial_1 = \bar{\partial} + \partial. \quad (1.11)$$

The energy E and momentum k can be written in terms of the light-cone spectral parameter ζ,

$$k = \frac{1}{2}\left(\zeta - \frac{1}{\zeta}\right), \qquad E = -\frac{1}{2}\left(\zeta + \frac{1}{\zeta}\right), \quad (1.12)$$

where we measure energies and momenta in units of m, the dynamically generated fermion mass. We have included a minus sign in the definition of E since for the consistency condition we will be summing over negative energy states in the Dirac sea. The various regions of the spectral plane, with corresponding energy and momentum, are shown in Fig. 1.

The boost parameter η, rapidity ξ, and velocity v are related by

$$\eta = e^{\xi} = \sqrt{\frac{1+v}{1-v}}, \qquad v = \frac{\eta^2 - 1}{\eta^2 + 1}. \quad (1.13)$$

Under a Lorentz boost, the light-cone variables transform as

$$z \to \eta z, \qquad \bar{z} \to \eta^{-1}\bar{z}, \qquad \zeta \to \eta\zeta, \quad (1.14)$$

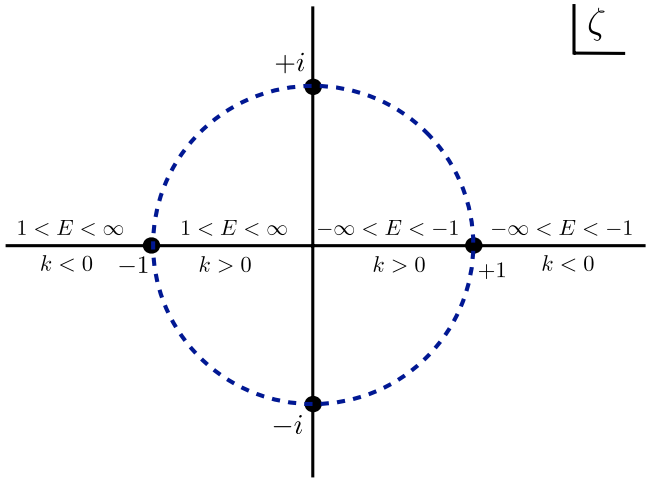

FIG. 1 (color online). The spectral ζ plane, indicating the regions of positive and negative energy and momentum. We have set the mass scale $m = 1$. Note that for ζ outside the unit circle the boost has a positive velocity, negative inside the unit circle. Bound states, having $|E| < 1$, correspond to a ζ of magnitude 1, lying on the unit circle.

and the Lorentz scalar argument of a plane wave is written as

$$k_\mu x^\mu = -\frac{1}{2}\left(\zeta\bar{z} - \frac{z}{\zeta}\right). \quad (1.15)$$

In terms of these variables, and in terms of the complex condensate (1.5), the Dirac equation for the two-component spinor ($\psi_1 = \psi_L$, $\psi_2 = \psi_R$) reads

$$2i\bar{\partial}\psi_2 = \Delta\psi_1, \qquad 2i\partial\psi_1 = -\Delta^*\psi_2. \quad (1.16)$$

II. GENERAL TDHF SOLUTION

A. Transparent potential

In a recent paper, a large class of transparent, time-dependent, scalar-pseudoscalar Dirac potentials was constructed [31]. The method used was a generalization of the method invented by Kay and Moses for finding all static, transparent Schrödinger potentials [39]. We collect the main results, referring to Ref. [31] for proofs and more details. We make the following ansatz for the continuum spinor:

$$\psi_\zeta = \frac{1}{\sqrt{1+\zeta^2}}\begin{pmatrix}\zeta\chi_1 \\ -\chi_2\end{pmatrix} e^{i(\zeta\bar{z} - z/\zeta)/2}, \quad (2.1)$$

where χ_1 and χ_2 approach some constant for $x \to \infty$. In that case, the continuum spinor behaves like a plane wave traveling to the right for $x \to -\infty$, as well as for $x \to \infty$ (for $k > 0$); hence, it is manifestly reflectionless.

The basic ingredients in the construction of Δ and ψ_ζ are N "plane wave" factors e_n, f_n, with complex spectral parameters ζ_n,

$$e_n = e^{i(\zeta_n^*\bar{z} - z/\zeta_n^*)/2}, \quad f_n = \frac{e_n}{\zeta_n^*}, \quad n = 1, \ldots, N. \quad (2.2)$$

N is the number of bound states. The reduced spinor components $\chi_{1,2}$ in Eq. (2.1) are written as finite sums with N poles:

$$\chi_1 = 1 + i\sum_{n=1}^{N}\frac{1}{\zeta - \zeta_n}e_n^*\varphi_{1,n}, \quad \chi_2 = 1 - i\sum_{n=1}^{N}\frac{\zeta}{\zeta - \zeta_n}e_n^*\varphi_{2,n}. \quad (2.3)$$

Here $\varphi_{1,n}$ and $\varphi_{2,n}$ are $2N$ functions defined as the solutions of the following systems of *linear, algebraic* equations,

$$\sum_{m=1}^{N}(\omega + B)_{nm}\varphi_{1,m} = e_n, \quad \sum_{m=1}^{N}(\omega + B)_{nm}\varphi_{2,m} = -f_n. \quad (2.4)$$

Here, ω is a constant, Hermitian, but otherwise arbitrary $N \times N$ matrix, and B is an $N \times N$ matrix constructed from

the basis functions, $e_n(z,\bar{z})$, and spectral parameters, ζ_n, as follows:

$$B_{nm} = i\frac{e_n e_m^*}{\zeta_m - \zeta_n^*}. \tag{2.5}$$

The ζ_n can be identified with the positions of the bound state poles of ψ_ζ in the complex ζ plane; see Eq. (2.3). To simplify the notation, we denote by e, f, φ_1, φ_2 the N-dimensional vectors with components e_n, f_n, $\varphi_{1,n}$, $\varphi_{2,n}$, respectively, whereas ω and B denote $N \times N$ matrices. Equation (2.4) becomes

$$(\omega + B)\varphi_1 = e, \qquad (\omega + B)\varphi_2 = -f. \tag{2.6}$$

As shown in Ref. [31], the φ_n are N bound state spinors, and ψ_ζ is the continuum spinor belonging to the transparent Dirac potential

$$\Delta = 1 - ie^\dagger\varphi_2 = 1 + i\varphi_1^\dagger f = 1 + ie^\dagger\frac{1}{\omega + B}f. \tag{2.7}$$

The three different expressions for Δ given here are equivalent owing to Eq. (2.6). Let us introduce a third vector g in addition to e, f defined in Eq. (2.2), with components

$$g_n = \frac{e_n}{\zeta - \zeta_n^*}. \tag{2.8}$$

This yields more compact expressions for χ_1, χ_2 as well,

$$\chi_1 = 1 + ig^\dagger\varphi_1, \qquad \chi_2 = 1 - i\zeta g^\dagger\varphi_2. \tag{2.9}$$

Furthermore, simple expressions in terms of determinants were presented in Refs. [24,31] for the condensate Δ and the spinor components $\chi_{1,2}$.

The bound state spinors φ_n are in general neither orthogonal nor normalized. A set of properly orthonormalized spinors can be constructed via

$$\hat{\varphi}_n = \sum_{m=1}^{N} C_{nm}\varphi_m, \qquad \int_{-\infty}^{\infty} dx\hat{\varphi}_n^\dagger\hat{\varphi}_m = \delta_{n,m}. \tag{2.10}$$

As shown in Ref. [31], the matrix C then satisfies the condition

$$2C\omega^{-1}C^\dagger = 1. \tag{2.11}$$

This was derived under the assumption that $\mathrm{Im}\, k_n > 0$, where

$$k_n = \frac{1}{2}\left(\zeta_n - \frac{1}{\zeta_n}\right) \tag{2.12}$$

is the complex momentum belonging to the nth bound state. The following asymptotic behavior of the potential was found in Ref. [31]:

$$\lim_{x\to-\infty}\Delta = 1, \qquad \lim_{x\to\infty}\Delta = \prod_{n=1}^{N}\frac{\zeta_n}{\zeta_n^*} = e^{i\Theta}. \tag{2.13}$$

This shows that Δ has a chiral twist $e^{i\Theta}$, where the chiral twist angle Θ can be computed by simply adding up the phases of all bound state pole parameters ζ_n,

$$\Theta = 2\sum_{n=1}^{N}\theta_n, \qquad \zeta_n = |\zeta_n|e^{i\theta_n}. \tag{2.14}$$

The spinor components have the asymptotic behavior

$$\lim_{x\to-\infty}\chi_1 = 1, \qquad \lim_{x\to\infty}\chi_1 = \prod_{n=1}^{N}\frac{\zeta - \zeta_n^*}{\zeta - \zeta_n}, \tag{2.15}$$

$$\lim_{x\to-\infty}\chi_2 = 1, \qquad \lim_{x\to\infty}\chi_2 = \prod_{n=1}^{N}\frac{\zeta_n}{\zeta_n^*}\frac{\zeta - \zeta_n^*}{\zeta - \zeta_n}. \tag{2.16}$$

From Eq. (2.15) we can read off the fully factorized, unitary transmission amplitude $T(\zeta)$ with the expected pole structure,

$$T(\zeta) = \prod_{n=1}^{N}\frac{\zeta - \zeta_n^*}{\zeta - \zeta_n}, \qquad |T(\zeta)| = 1. \tag{2.17}$$

The extra factors in the product in Eq. (2.16) are due to the chiral twist of the potential Δ, which also affects the spinors.

B. Self-consistency

We now show that this solution also gives a self-consistent solution to the fully quantized TDHF problem (1.4), provided certain filling-fraction conditions are satisfied by the combined soliton-fermion system, generalizing the conditions already found by DHN and Shei [22,32]. The TDHF potential Δ receives contributions from the Dirac sea and the valence bound states,

$$\Delta = -2Ng^2(\langle\psi_1^*\psi_2\rangle_{\mathrm{sea}} + \langle\psi_1^*\psi_2\rangle_{\mathrm{b}}), \tag{2.18}$$

with

$$\langle\psi_1^*\psi_2\rangle_{\mathrm{sea}} = -\frac{1}{2}\int_{1/\Lambda}^{\Lambda}\frac{d\zeta}{2\pi}\frac{1}{\zeta}\chi_1^*\chi_2, \tag{2.19}$$

$$\langle\psi_1^*\psi_2\rangle_{\mathrm{b}} = \sum_n \nu_n\hat{\varphi}_{1,n}^*\hat{\varphi}_{2,n}. \tag{2.20}$$

The integration limits in Eq. (2.19) correspond to a symmetric momentum cutoff $\pm\Lambda/2$ in ordinary coordinates. We insert the expressions for χ_1, χ_2 from Eq. (2.9) and isolate the ζ dependence of the integrand in the continuum

part (2.19). The integrand contains only simple poles in the complex ζ plane, so that the integration over $d\zeta$ with a cutoff can easily be performed. The pole at $\zeta = 0$ yields the divergent contribution

$$\langle \psi_1^* \psi_2 \rangle_{\rm sea}|_{\rm div} = -\frac{\Delta}{2\pi} \ln \Lambda. \tag{2.21}$$

If one inserts this into Eq. (2.18) and uses the vacuum gap equation

$$\frac{Ng^2}{\pi} \ln \Lambda = 1, \tag{2.22}$$

one finds that this part gives self-consistency by itself. Requiring that the convergent part of the sea contribution cancels the bound state contribution should give us the relationship between the bound state occupation fractions ν_n and the parameters of the solution, provided the solution is self-consistent. The computation of the convergent part of the sea contribution is straightforward. To present the result in a concise form, we introduce a diagonal matrix M,

$$M_{nm} = -i\delta_{nm} \ln(-\zeta_n^*). \tag{2.23}$$

(Logarithms of ζ_n appear if one integrates over $d\zeta$, as a result of the simple poles in the complex ζ plane.) The convergent part of Eq. (2.19) can then be simplified to

$$\langle \psi_1^* \psi_2 \rangle_{\rm sea}|_{\rm conv} = -\frac{1}{4\pi} \varphi_1^\dagger (\omega M^\dagger + M\omega)\varphi_2. \tag{2.24}$$

The bound state contribution (2.20) is evaluated with the help of Eq. (2.11). After introducing another diagonal matrix N,

$$N_{nm} = 4\pi \delta_{nm} \nu_n, \tag{2.25}$$

it can be written as

$$\langle \psi_1^* \psi_2 \rangle_{\rm b} = \frac{1}{4\pi} \varphi_1^\dagger (C^\dagger N C)\varphi_2. \tag{2.26}$$

Expressions (2.24) and (2.26) cancel if we require that

$$\omega M^\dagger + M\omega = C^\dagger N C. \tag{2.27}$$

This is the self-consistency relation determining the bound state occupation fractions. It can be cast into a more convenient form by combining Eqs. (2.11) and (2.27) as follows. From our experience with concrete applications of this formalism, it appears that ω should be chosen as a positive definite matrix to avoid singularities in Δ as a function of (x, t). Assuming that ω is positive definite, it has the unique Cholesky decomposition

$$\omega = LL^\dagger, \tag{2.28}$$

where L is a lower triangular matrix. From Eq. (2.11) we conclude that the matrix

$$V = \sqrt{2} C \frac{1}{L^\dagger} \tag{2.29}$$

is unitary. The self-consistency condition (2.27) can then be transformed into the final form

$$2\left(L^\dagger M^\dagger \frac{1}{L^\dagger} + \frac{1}{L} M L \right) = V^\dagger N V. \tag{2.30}$$

Thus, the eigenvalues of the matrix on the left-hand side of Eq. (2.30) determine the diagonal entries of the matrix N, which yield the fermion filling fractions ν_n in Eq. (2.25). To test whether a given candidate solution is self-consistent, one has to confirm that all eigenvalues are between 0 and 4π, thereby satisfying the self-consistency condition with physical occupation fractions $\nu_n \in [0, 1]$. As an alternative to the Cholesky decomposition, Eq. (2.30) remains valid if one replaces L by $\sqrt{\omega}$, which can be computed by diagonalizing ω first.

C. Vanishing fermion density

Because of strong constraints from chiral symmetry in $1 + 1$ dimensions, the massless NJL$_2$ model does not allow any localized fermion density or current [40]. Similarly, there is no localized energy or momentum density [41]. This follows from the conservation laws

$$\partial_\mu j_V^\mu = 0, \qquad \partial_\mu j_A^\mu = 0, \qquad \partial_\mu \mathcal{T}^{\mu\nu} = 0 \tag{2.31}$$

together with the fact that

$$\begin{aligned} j_V^0 &= j_A^1 = \psi^\dagger \psi, \qquad & j_V^1 &= j_A^0 = \psi^\dagger \gamma_5 \psi \\ \mathcal{T}^{00} &= \mathcal{T}^{11} = \mathcal{H}, \qquad & \mathcal{T}^{01} &= \mathcal{T}^{10} = \mathcal{P} \end{aligned} \tag{2.32}$$

in the massless NJL$_2$ model. The conservation laws (2.31) remain valid in TDHF approximation. Since the bound states carry lumps of localized fermions, there must be an exact cancellation between continuum states and bound states for all of these densities. As a consistency test of the above TDHF solution, let us check this cancellation explicitly for the simplest case, the fermion density $\rho = j_V^0$. The induced fermion density in the Dirac sea is

$$\begin{aligned} \rho_{\rm ind} &= \int_0^\infty \frac{d\zeta}{2\pi} \frac{\zeta^2 + 1}{2\zeta^2} (\psi_\zeta^\dagger \psi_\zeta - 1) \\ &= \frac{1}{2} \int_0^\infty \frac{d\zeta}{2\pi} \left\{ |\chi_1|^2 - 1 + \frac{1}{\zeta^2} (|\chi_2|^2 - 1) \right\}. \end{aligned} \tag{2.33}$$

If we replace χ_1, χ_2 by the expressions given in Eq. (2.9), we can simplify the result after some straightforward computations to

$$\rho_{\rm ind} = \partial_x \int_0^\infty \frac{d\zeta}{2\pi} g^\dagger \frac{1}{\omega + B} g. \tag{2.34}$$

Inserting the g's and performing the integration over $d\zeta$, the result can be written as

$$\rho_{\mathrm{ind}} = \frac{1}{2\pi}\,\mathrm{Tr}\left[(\omega M^\dagger + M\omega)\partial_x \frac{1}{\omega + B}\right]. \tag{2.35}$$

The density from the bound states with occupation fractions ν_n yields [31]

$$\rho_b = \sum_n \nu_n \hat{\varphi}_n^\dagger \hat{\varphi}_n = -\frac{1}{2\pi}\,\mathrm{Tr}\left[(C^\dagger N C)\partial_x \frac{1}{\omega + B}\right]. \tag{2.36}$$

If the self-consistency condition (2.27) is satisfied, the bound state density (2.36) and the induced fermion density in the sea (2.35) cancel exactly. The vanishing of the current density j_V^1 can be proven in a similar manner, the only difference being that ∂_x gets replaced by ∂_t everywhere.

D. Time delays and masses

In standard soliton theory, the outcome of a scattering process is expressed via the time delay experienced by the solitons during the collision. As already discussed in Ref. [38], the situation is more complicated if multisoliton bound states are involved. In this case the shape of the bound state may be affected as well. In the present work, we face the additional complication that the phases entering the breather oscillation may be changed during the scattering process. The best way to define the outcome of such a scattering process of composite multisoliton objects is to compare the potential Δ for a cluster of kinks moving with a common velocity v_0 before and after the collision. Inspection of a few cases with small number of kinks shows the following general pattern: The change in Δ for a cluster involving K kinks consists of an overall twist factor τ and rescalings of all the elementary functions e_n by complex numbers λ_n,

$$\Delta_{\mathrm{out}}(e_{i_1}, \ldots, e_{i_K}) = \tau \Delta_{\mathrm{in}}(\lambda_{i_1} e_{i_1}, \ldots, \lambda_{i_K} e_{i_K}), \tag{2.37}$$

with

$$\tau = \prod_{n(v_n<v_0)} \frac{\zeta_n}{\zeta_n^*} \prod_{m(v_m>v_0)} \frac{\zeta_m^*}{\zeta_m},$$
$$\lambda_n = \prod_{m(v_m<v_0)} \left(\frac{\zeta_n^* - \zeta_m^*}{\zeta_n^* - \zeta_m}\right) \prod_{k(v_k>v_0)} \left(\frac{\zeta_n^* - \zeta_k}{\zeta_n^* - \zeta_k^*}\right). \tag{2.38}$$

Alternatively, one could interpret the rescalings of the e_n as a modification of the matrix ω^0 of the cluster (one block out of the full, block-diagonal matrix ω),

$$\omega^0_{nm}|_{\mathrm{out}} = \frac{\omega^0_{nm}|_{\mathrm{in}}}{\lambda_n \lambda_m^*}. \tag{2.39}$$

The twist factor τ can readily be understood in terms of the chiral twists of the solitons involved in the scattering process. The elementary factors entering the expression for λ_n also have a simple interpretation. The transmission amplitude of a fermion with spectral parameter ζ scattering off soliton m is

$$T_m(\zeta) = \frac{\zeta - \zeta_m^*}{\zeta - \zeta_m}. \tag{2.40}$$

Hence, the factor λ_n in Eq. (2.38) can be expressed in terms of transmission amplitudes of a fermion on all solitons not belonging to the cluster, evaluated at the complex spectral parameter ζ_n^*, the complex conjugate of the bound state pole position,

$$\lambda_n = \prod_{m(v_m<v_0)} T_m(\zeta_n^*) \prod_{k(v_k>v_0)} \frac{1}{T_k(\zeta_n^*)}. \tag{2.41}$$

Another question of interest concerns the masses of clusters of solitons. In Ref. [41], a formula for the mass of TDHF solutions of the NJL_2 model was derived. Starting from Eqs. (2.31) and (2.32) for the energy momentum tensor, it was found that the mass can be expressed in terms of the asymptotic behavior of the fermion phase shift for $k \to \infty$,

$$M = \frac{N}{\pi} \lim_{k\to\infty} k\delta(k). \tag{2.42}$$

Here, $\delta(k)$ is the phase of the (unimodular) fermion transmission amplitude $T(k)$. For a single twisted kink, this reproduces the original result of Shei [32]:

$$M_1 = \frac{N}{\pi} \sin\phi_1, \qquad \zeta_1 = -e^{-i\phi_1}. \tag{2.43}$$

According to Eq. (2.17), the full transmission amplitude factorizes into fermion-kink transition amplitudes; hence, the phase shifts are additive, as expected for integrable systems. This holds independently of whether the solitons form static bound states or breathers. Consequently, the mass of any compound of n solitons is just the sum of the masses of the constituents—the binding energy vanishes. This is consistent with what has already been known for static bound states since Ref. [32] but generalizes to the breather case as well.

An interesting spinoff results if we apply these insights to real Δ, i.e., TDHF solutions of the GN model. A 2-kink bound state has the mass

$$M_{\mathrm{kink}}(\phi_1) + M_{\mathrm{kink}}(\pi - \phi_1) = \frac{2N}{\pi} \sin\phi_1. \tag{2.44}$$

This relates the mass of the DHN baryon (or breather, for that matter) to the mass of the Shei kink ($\sin\phi_1$ is the parameter y in DHN). This is perhaps the most conspicuous

manifestation of the long-overlooked fact that twisted kinks are the (hidden) constituents of the DHN baryon.

III. EXPLICIT EXAMPLES

In this section we illustrate the general solution to the TDHF problem (2.7), (2.9), (2.30) with several examples. We classify the applications according to the number of bound states or, equivalently, the number of poles of the continuum spinors in the complex ζ plane.

A. General solution with one pole: twisted kink

With one pole, the matrix ω is just a real number, and the matrix B reduces to a single function of z, $\bar{z}$. We parametrize the position ζ_1 of the pole as

$$\zeta_1 = -\frac{e^{-i\phi_1}}{\eta_1}, \qquad \eta_1 = \sqrt{\frac{1+v_1}{1-v_1}}. \tag{3.1}$$

The complex potential Δ can then be written as

$$\Delta = \frac{1+e^{-2i\phi_1}U_1}{1+U_1} \tag{3.2}$$

with the real function

$$U_1 = \frac{B_{11}}{\omega_{11}} = \frac{\eta_1}{2\omega_{11}\sin\phi_1}\exp\left\{\frac{\sin\phi_1}{\eta_1}(\bar{z}+\eta_1^2 z)\right\}. \tag{3.3}$$

Expressed in ordinary coordinates, the argument of the exponential in U_1 reads

$$\frac{\sin\phi_1}{\eta_1}(\bar{z}+\eta_1^2 z) = 2\sin\phi_1\frac{x-v_1 t}{\sqrt{1-v_1^2}}. \tag{3.4}$$

This is the boosted form of the Shei twisted kink (1.7) for the NJL_2 model. The role of the free parameter ω_{11} is to shift the position of the kink. The phase and modulus of ζ_1 are related to the chiral twist and the velocity of the kink, respectively, as illustrated in Fig. 2. To cover the full range of chiral twists, it is sufficient to restrict ϕ_1 to the interval $[0,\pi]$. In this case, $\sin\phi_1 > 0$, and we have to choose $\omega_{11} > 0$ in order to get a nonsingular Δ. Notice that this definition of ϕ_1 also implies $\mathrm{Im}\, k_1 > 0$, as assumed in Ref. [31]. Turning to the self-consistency issue, the matrix M introduced in Eq. (2.23) has just one component: $M_{11} = -i\ln(-\zeta_1^*) = \phi_1 + i\ln\eta_1$. Thus, the NJL_2 filling-fraction condition (2.30) gives

$$\nu_1 = \frac{\phi_1}{\pi}, \tag{3.5}$$

This self-consistent TDHF kink binds a number n_v of valence fermions, where in the large N_f limit the filling fraction $\nu_1 = n_v/N_f$ is equal to the twist angle ϕ_1 divided by π.

We obtain the real kink solution (1.6) of GN_2 by choosing $\phi_1 = \frac{\pi}{2}$ in Eqs. (3.2) and (3.3). For GN_2 there is no filling fraction condition, as we do not have to impose a self-consistency condition on the pseudoscalar condensate.

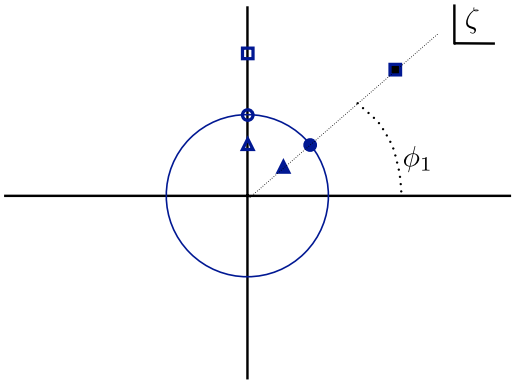

FIG. 2 (color online). A spectral ζ plane representation of single kinks. Each of the open square, circle, and triangle on the positive imaginary axis represents a real GN_2 kink, with positive, zero, or negative boost, with respect to the rest frame. Each of the full square, circle, and triangle on the ray at angle φ_1 represents a complex twisted NJL_2 kink with phase parameter φ_1. Taken together, all these six points represent the scattering of six kinks, three of them real and three with (equal) twist parameter φ_1.

In an (S,P) plot, the twisted kink traces out a segment of a straight line, joining two points on the chiral circle. In our case, the starting point $(x \to -\infty)$ is always the point $(S=1,\ P=0)$, whereas the end point $(x \to \infty)$ depends on the chiral twist. Most of the examples discussed below are based on constituent kinks with parameters $\phi_1 = 1.0,\ 0.8,\ 0.6,\ 0.4$, shown in Fig. 3 and, in greater detail, in the Supplemental Material [42] to this paper (see 3dplot_constituent_kinks).

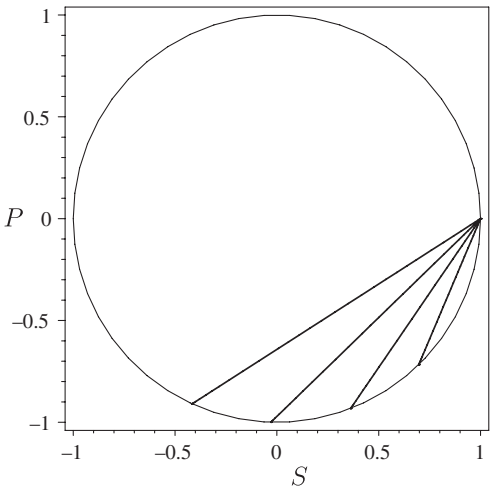

FIG. 3. (S,P) plot, of the scalar (S) and pseudoscalar (P) components of the condensate Δ, for the four basic twisted kinks used to build up most of the multikink configurations in this work, as explained in the text.

B. General solution with two poles: kinks, baryons, and breathers

With two poles, the matrices entering the general solution (2.7), (2.9), (2.30) are 2×2. This enables us to work out everything explicitly, including the self-consistency condition. The physics depends on the assumptions about the constant matrix ω and the pole positions $\zeta_{1,2}$.

1. Nonbreather solutions

We find nonbreather solutions by choosing a diagonal form of ω in Eq. (2.7). Introducing functions $U_i = B_{ii}/\omega_{ii}$ for $i = 1, 2$ in analogy to Eq. (3.3) and generalizing the parametrization (3.1) to $\zeta_{1,2}$, we find the potential

$$\Delta = \frac{1 + e^{-2i\phi_1}U_1 + e^{-2i\phi_2}U_2 + b_{12}e^{-2i(\phi_1+\phi_2)}U_1U_2}{1 + U_1 + U_2 + b_{12}U_1U_2}. \tag{3.6}$$

The interaction effects between the two twisted kinks are described by the real parameter b_{12} given by

$$b_{12} = \left|\frac{\zeta_1 - \zeta_2}{\zeta_1 - \zeta_2^*}\right|^2 = \frac{\eta_1^2 + \eta_2^2 - 2\eta_1\eta_2\cos(\phi_1 - \phi_2)}{\eta_1^2 + \eta_2^2 - 2\eta_1\eta_2\cos(\phi_1 + \phi_2)}. \tag{3.7}$$

This is the $N = 2$ case of a general formula valid for diagonal ω, presented in Sec. 3B of Ref. [31]. Equation (3.6) gives the self-consistent potential for the scattering of two twisted kinks, with twist angles ϕ_1 and ϕ_2 and boost parameters η_1 and η_2, or for a bound state if one chooses $\eta_1 = \eta_2$. The filling-fraction consistency condition is simple when ω is diagonal. The M matrix is $M = \mathrm{diag}(\phi_1 + i\ln\eta_1, \phi_2 + i\ln\eta_2)$. Thus, we find filling fractions

$$\nu_1 = \frac{\phi_1}{\pi}, \qquad \nu_2 = \frac{\phi_2}{\pi}, \tag{3.8}$$

as expected from the asymptotics of the scattering problem. If we are interested in solutions of the NJL_2 model with real Δ, we are restricted to fermion number 0. In that case the self-consistency condition yields

$$\nu_1 = \frac{\phi_1}{\pi}, \qquad \nu_2 = \frac{\phi_2}{\pi} = \frac{\pi - \phi_1}{\pi} = 1 - \nu_1. \tag{3.9}$$

This corresponds to an "exciton" in condensed matter language. In the GN case, we cannot take over the derivation of the self-consistency condition, which was only valid for generic parameters. Now, the contributions of the 2 bound states give equal and opposite contributions to the condensate $\bar{\psi}\psi$, so that only the difference of the corresponding two equations of the NJL_2 model survives,

$$\nu_1 - \nu_2 = \frac{\phi_1 - \phi_2}{\pi} = \frac{2\phi_1}{\pi} - 1. \tag{3.10}$$

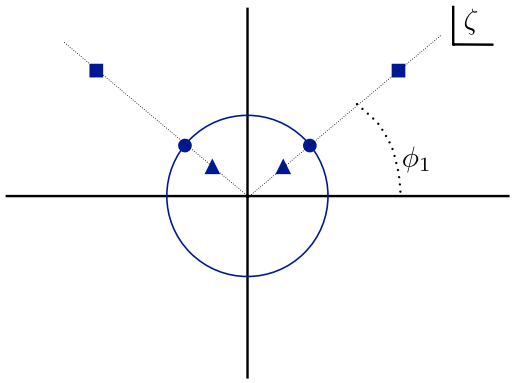

FIG. 4 (color online). A spectral ζ plane representation of a real GN_2 baryon. The baryon is composed of two twisted kinks, one with chiral angle φ_1 and the other with $\pi - \varphi_1$. The triangles (squares) have $\zeta_1 < 1$ ($\zeta_1 > 1$), corresponding to negative (positive) boost parameter, while the circles correspond to a baryon at rest.

The baryon state of lowest energy for a given baryon number has fully occupied the negative energy bound state, corresponding to $\nu_2 = 1, \nu_1 = 2\phi_1/\pi$. This is the relation familiar from DHN.

We can consider various special cases:

1. Scattering of two GN_2 kinks. We obtain real kink solutions by setting $\phi_1 = \phi_2 = \frac{\pi}{2}$. Then

$$S = \frac{1 - U_1 - U_2 + b_{12}U_1U_2}{1 + U_1 + U_2 + b_{12}U_1U_2}, \qquad b_{12} = \left(\frac{\eta_1 - \eta_2}{\eta_1 + \eta_2}\right)^2, \tag{3.11}$$

and $\sin\phi_{1,2} = 1$ in the definition of $U_{1,2}$. This agrees with the $n = 2$ case of the general formula in Ref. [29]. There is no filling-fraction consistency condition.

2. GN_2 baryon. We can also obtain a real solution by choosing $\phi_2 = \pi - \phi_1$, together with $\omega_{11} = \omega_{22}$. To obtain a baryon, we also choose $\eta_1 = \eta_2$. Then $U_1 = U_2$, and we find

$$S = \frac{1 + 2\cos(2\phi_1)U_1 + \cos^2\phi_1 U_1^2}{1 + 2U_1 + \cos^2\phi_1 U_1^2}, \tag{3.12}$$

which agrees with the GN_2 baryon in Eq. (1.8). Thus, we see that the DHN GN_2 baryon is in fact a bound pair of two twisted kinks, as depicted in Fig. 4. The fermion filling fractions are $\nu_2 = 1$, $\nu_1 = 2\phi_1/\pi$, as in DHN. Note that DHN have written the parameter y, which defines the size of the baryon in the form $y = \sin\theta$, without geometrical interpretation of the angle θ. Now we see that θ is nothing but the angle ϕ_1 related to the twist of the constituent kinks. These constituents are well hidden inside the baryon, since the individual twisted kinks are not solutions of the GN model. The only observable which hints at this compositeness is the factorized fermion transmission amplitude.

2. Breather solutions

Breather solutions in the rest frame are obtained by choosing $\eta_1 = \eta_2 = 1$ and a nondiagonal 2×2 matrix ω in Eqs. (2.14) and (2.30). Using the freedom of making translations in x and t, we choose the following positive definite Hermitian matrix:

$$\omega = \begin{pmatrix} \sec\chi & \tan\chi \\ \tan\chi & \sec\chi \end{pmatrix}. \tag{3.13}$$

Then we find for the GN_2 system, where $\phi_2 = \pi - \phi_1$,

$$\begin{aligned} S &= \frac{\mathcal{N}}{\mathcal{D}} \\ \mathcal{N} &= 1 + \frac{\cos(2\phi_1)}{\sin\phi_1 \cos\chi} e^{2x \sin\phi_1} \\ &\quad + \tan\chi e^{2x \sin\phi_1} \sin(2t\cos\phi_1 + \phi_1) \\ &\quad + \frac{1}{4}\cot^2\phi_1 e^{4x\sin\phi_1} \\ \mathcal{D} &= 1 + \frac{1}{\sin\phi_1\cos\chi} e^{2x\sin\phi_1} \\ &\quad - \tan\chi e^{2x\sin\phi_1} \sin(2t\cos\phi_1 + \phi_1) \\ &\quad + \frac{1}{4}\cot^2\phi_1 e^{4x\sin\phi_1}. \end{aligned} \tag{3.14}$$

This agrees (modulo translations in x and t) with the DHN GN_2 breather (1.9) if we use the following identifications:

$$\epsilon = \tan\phi_1, \quad b = \frac{1}{\cos\phi_1\cos\chi}, \quad a = \tan\phi_1\tan\chi. \tag{3.15}$$

The limit $\chi \to 0$ of Eq. (3.14) yields back the static DHN baryon (3.12) up to a shift in x, as can be seen by setting

$$U_1 = \frac{e^{2x\sin\phi_1}}{2\sin\phi_1}. \tag{3.16}$$

A new twisted breather for the NJL_2 model is obtained by choosing the off-diagonal mixing matrix (3.13) and relaxing the reality condition (so that $\phi_2 \neq \pi - \phi_1$) on the twist angles. This is the most complicated TDHF solution with two poles. To exhibit its structure, we first write down the potential Δ in the form

$$\begin{aligned} \Delta &= \frac{\mathcal{N}}{\mathcal{D}} \\ \mathcal{N} &= 1 + \frac{1}{\cos\chi}\left(\frac{\zeta_1}{\zeta_1^*}U_1 + \frac{\zeta_2}{\zeta_2^*}U_2\right) + b_{12}\frac{\zeta_1\zeta_2}{\zeta_1^*\zeta_2^*}U_1U_2 \\ &\quad - \tan\chi\left(\frac{\zeta_2}{\zeta_1^*}B_{12} + \frac{\zeta_1}{\zeta_2^*}B_{21}\right) \\ \mathcal{D} &= 1 + \frac{1}{\cos\chi}(U_1 + U_2) + b_{12}U_1U_2 - \tan\chi(B_{12} + B_{21}) \end{aligned} \tag{3.17}$$

with $U_1 = B_{11}$, $U_2 = B_{22}$, B_{nm} from Eq. (2.5), and b_{12} from Eq. (3.7). In the limit $\chi \to 0$, we recover the bound state of twisted kinks; see Eq. (3.6). The chiral twist of the solution is time independent and can be inferred from the prefactors of the U_1U_2 terms. It does not depend on χ and therefore coincides with the sum of the individual twists, like for the bound state. Consider the oscillating terms in $\mathcal{N}$ and $\mathcal{D}$ first, i.e., those multiplied by $\tan\chi$. Using ordinary coordinates to exhibit their space and time dependence, the factors multiplying $\tan\chi$ can be cast into the form

$$\begin{aligned} \left(\frac{\zeta_2}{\zeta_1^*}B_{12} + \frac{\zeta_1}{\zeta_2^*}B_{21}\right) &= e^{-i(\phi_1+\phi_2)}(B_{12} + B_{21}), \\ (B_{12} + B_{21}) &= -\frac{2e^{Kx}}{\sqrt{K^2+\Omega^2}} \sin\left(\Omega t + \arctan\frac{K}{\Omega}\right), \end{aligned} \tag{3.18}$$

where we have introduced a wave number K and frequency Ω generalizing the corresponding quantities from the (real) DHN breather,

$$K = \sin\phi_1 + \sin\phi_2, \quad \Omega = \cos\phi_1 - \cos\phi_2. \tag{3.19}$$

The period of the twisted breather is $T = 2\pi/\Omega$. The time-independent parts of $\mathcal{N}$ and $\mathcal{D}$ can be evaluated with the help of

$$\begin{aligned} U_1 &= \frac{e^{2x\sin\phi_1}}{2\sin\phi_1}, \qquad U_2 = \frac{e^{2x\sin\phi_2}}{2\sin\phi_2}, \\ b_{12} &= \frac{1-\cos(\phi_1-\phi_2)}{1-\cos(\phi_1+\phi_2)}. \end{aligned} \tag{3.20}$$

Let us now turn to the issue of self-consistency. Following the steps leading to Eq. (2.30), we write ω in its Cholesky factorized form:

$$\begin{aligned} \omega &= \begin{pmatrix} \sec\chi & \tan\chi \\ \tan\chi & \sec\chi \end{pmatrix} = LL^\dagger, \\ L &= \begin{pmatrix} \sqrt{\sec\chi} & 0 \\ \sqrt{\cos\chi}\tan\chi & \sqrt{\cos\chi} \end{pmatrix}. \end{aligned} \tag{3.21}$$

Then

$$\begin{aligned} &2\left(L^\dagger M^\dagger \frac{1}{L^\dagger} + \frac{1}{L}ML\right) \\ &= 2\begin{pmatrix} 2\phi_1 & -(\phi_1-\phi_2)\tan\chi \\ -(\phi_1-\phi_2)\tan\chi & 2\phi_2 \end{pmatrix}. \end{aligned} \tag{3.22}$$

Using Eq. (2.30), the eigenvalues of this matrix give the two filling fractions as

TABLE I. Summary of all two-pole solutions

ω	η	ϕ	Object
Diagonal	$\eta_1 = \eta_2$	$\phi_1 + \phi_2 = \pi$	DHN baryon
		$\phi_1 + \phi_2 \neq \pi$	Twisted kink bound state
	$\eta_1 \neq \eta_2$	$\phi_1 = \phi_2 = \pi/2$	CCGZ kink scattering
		other ϕ_i's	Twisted kink scattering
Off-diagonal	$\eta_1 = \eta_2$	$\phi_1 + \phi_2 = \pi$	DHN breather
		$\phi_1 + \phi_2 \neq \pi$	Twisted breather
	$\eta_1 \neq \eta_2$	all ϕ_i's	Unphysical

$$\nu_\pm = \frac{\phi_1 + \phi_2}{2\pi} \pm \frac{\phi_1 - \phi_2}{2\pi} \sec\chi. \tag{3.23}$$

The condition that $\nu_\pm \in [0, 1]$ restricts the allowed range of χ for given twist angles ϕ_1, ϕ_2.

Finally, the most general two-pole solution would seem to be the one with off-diagonal ω and $\eta_1 \neq \eta_2$, combining elements from the breather and the scattering problem. We have not considered this option for the following reason. As is clear from Eq. (2.11), a nondiagonal ω implies a nondiagonal matrix C. This in turn means that the bound states $\hat{\varphi}_n$ entering the TDHF problem are mixtures of kink bound states φ_1, φ_2 moving at different velocities; see Eq. (2.10). At asymptotic times we would then be dealing with superpositions of states located infinitely far apart, in violation of the principle of cluster separability. Although such solutions do exist mathematically, they would not correspond to any kind of observable scattering process, since the initial state could not be prepared. An overview over all the possibilities with two poles is given in Table 1, as a short summary of Sec. III B.

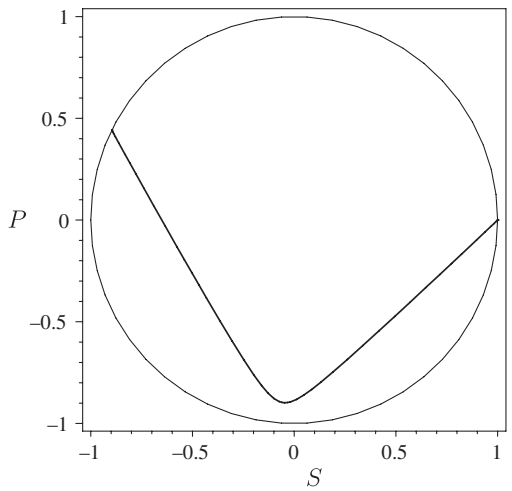

FIG. 5. (S, P) plot of a 2-kink, a bound state of two twisted kinks.

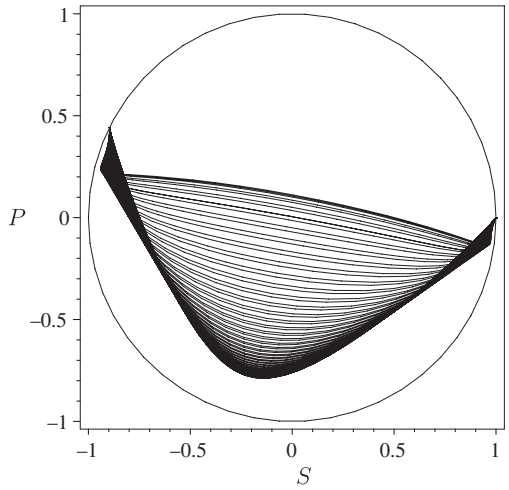

FIG. 6. (S, P) plot of a 2-breather made out of two kinks with the same parameters as the bound state in Fig. 5. The different curves illustrate the time dependence of the twisted breather, in equal time steps.

We illustrate these various examples in a few cases, using (S, P) plots. In Fig. 5, a 2-kink bound state at rest (parameters: $\phi_1 = 1.0$, $\phi_2 = 0.8$, $\omega_{11} = 3$, $\omega_{22} = 1/\omega_{11}$) is shown. If one increases the distance between the kinks by increasing ω_{11}, one reaches eventually two static, noninteracting kinks which would show up as an open polygon made out of two of the straight line segments shown in Fig. 3. The breather with the same parameters as the 2-kink and $\chi = 1.1$ is illustrated in Fig. 6, where the different curves correspond to equidistant time steps. Figure 7 shows the scattering of two twisted kinks with $\phi_1 = 1.0$, $\phi_2 = 0.8$. The initial and final states consist of two straight line segments ending on the chiral circle. During the

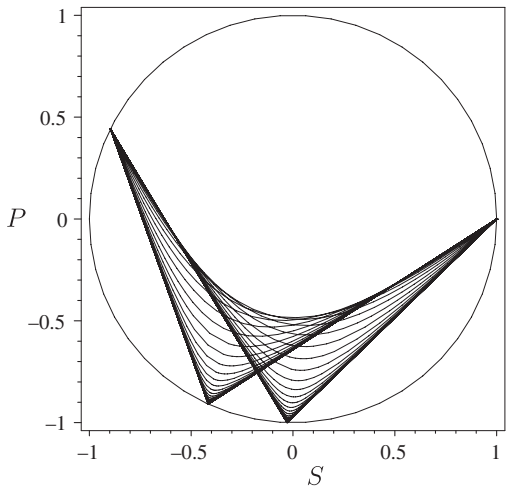

FIG. 7. (S, P) plot of the scattering process of two twisted kinks. The curves show the time dependence, in equal time steps. The initial and final states are open polygons with two segments, ending on the chiral circle.

collision process (illustrated again by a sequence of equidistant time steps), the kinks interchange their order. Clearly, these static pictures can give only an incomplete view of the time-dependent examples. A complete graphical representation requires animated plots, as provided in Ref. [42] for the same parameters; see the Appendix and the files ANIMATION_KINK_PLUS_KINK and ANIMATION_2-BREATHER.

C. Three-pole solutions

In the preceding section, we have discussed the TDHF solutions built out of two kinks in great detail. With an increasing number of kinks (or poles in the complex ζ plane), both the number of different physical configurations and the complexity of these solutions increase rapidly. It is straightforward to generate these solutions with computer algebra (CA) using the general formalism and to check the self-consistency by a numerical diagonalization of a finite matrix. We will show examples of such calculations at the end of this and the following sections. We start with a survey of the different cases with three poles.

The input to any TDHF calculation of the NJL_2 or GN models is a set of boost parameters η_n and chiral twist angles ϕ_n for the constituent kinks, together with the bound state mixing matrix ω. These parameters are not entirely independent, though. A nonvanishing off- diagonal matrix element ω_{nm} implies that the physical bound states of kinks n and m get mixed. This is only physically meaningful if these two kinks have the same boost parameter $\eta_n = \eta_m$, since otherwise the two kinks would be arbitrarily far apart at asymptotic times and the mixing would violate cluster separability. The other restriction is that two kinks (not involved in breathers) with the same η_n parameter must have different ϕ_n's; otherwise, the number of kinks is reduced by 1.

With this in mind, the possibilities with three kinks are as follows. If η_1, η_2, η_3 are all different, we are dealing with the scattering of three individual kinks. If one chooses in particular $\phi_n = \pi/2$ for all three kinks, this reproduces known results for three CCGZ kinks of the GN model derived from the Sinh–Gordon solitons in Ref. [29]. If two of the kinks have the same velocity (say $\eta_1 = \eta_2 \neq \eta_3$), we are dealing with the scattering of a 2-kink compound and a single kink, and we must choose $\omega_{13} = \omega_{23} = 0$. The compound system can either be a bound state ($\omega_{12} = 0$) or a breather ($\omega_{12} \neq 0$), as discussed in Sec. III B. In the case of real potentials, this includes scattering and bound states of a DHN breather or baryon ($\phi_2 = \pi - \phi_1$) and a CCGZ kink ($\phi_3 = \pi/2$). The bound state case has been discussed independently in the condensed matter [9] and particle physics [43] literature. Finally, if all three kinks have the same velocity, there are three possibilities for ω. First, if ω is diagonal, we describe the 3-kink bound state, which fits into the framework of Ref. [36]. Second, if only one off-diagonal element ω_{nm} is different from zero, this describes a bound state of a 2-kink breather (kinks n, m) and a single kink. Finally, if more than one off-diagonal element ω_{nm} is different from zero, this 3-kink compound state cannot be resolved into a 2-kink breather and a kink but represents a more complicated oscillation mode where all three kinks are involved in a nontrivial way. Of course, in all of these cases one has to check that the self-consistency condition can be fulfilled with physical occupation fractions $\nu_n \in [0, 1]$. Since this involves diagonalization of a 3×3 matrix, this has to be checked on a case-by-case basis.

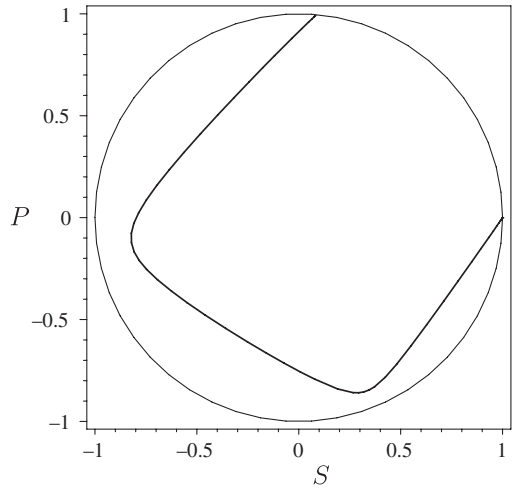

FIG. 8. (S, P) plot of a 3-kink, a bound state of three twisted kinks.

To simplify the discussion in the next section, we introduce the following language: A bound state of n twisted kinks will be referred to as "n-kink" (a "1-kink" being simply a kink). An irreducible breather made out of n kinks will be called "n-breather," If several clusters are scattering, this will be indicated by a + sign, e.g., kink + kink for the scattering of two kinks. Then the one-pole solution deals with the kink; the two-pole solution with kink + kink, 2-kink, and 2-breather; and the three-pole solution with kink+ kink + kink, kink + 2-kink, kink + 2-breather, 3-kink, and 3-breather.

Let us illustrate once again a few cases, using (S, P) plots. In Fig. 8, a 3-kink bound state at rest (parameters: $\phi_1 = 1.0$, $\phi_2 = 0.8$, $\phi_3 = 0.6$, $\omega_{11} = 9$, $\omega_{22} = 1$, $\omega_{33} = 1/9$) is shown. Figure 9 represents the scattering of a 2-kink bound state and a single kink ($\eta_1 = \eta_2 = 2, \eta_3 = 1/2$), and Fig. 10 represents the scattering of three twisted kinks ($\eta_1 = 2$, $\eta_2 = 1$, $\eta_3 = 1/2$). Similar plots involving 2-breathers or 3-breathers are not really able to convey a picture of the complicated time dependence. We refer the reader to the Appendix and Ref. [42], where full animations of all of these cases can be found (ANIMATION_KINK_PLUS_KINK_PLUS_KINK, ANIMATION_2-KINK_PLUS_KINK, ANIMATION_2-BREATHER_KINK_BOUNDSTATE, ANIMATION_2-BREATHER_PLUS_KINK, ANIMATION_3-BREATHER).

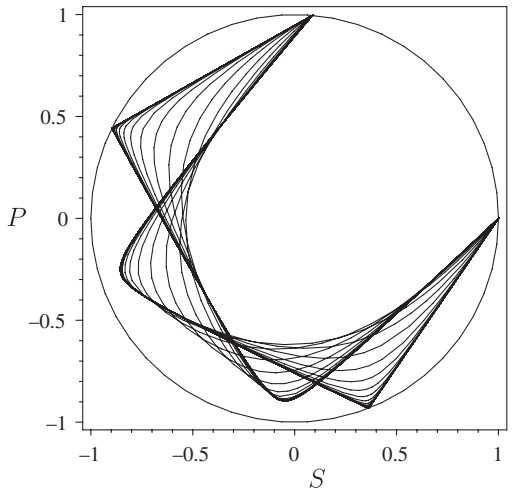

FIG. 9. (S, P) plot of the scattering of a 2-kink and a kink. The curves illustrate the time dependence, in equal time steps. Initial and final states can be identified by the fact that one inner point on a curve touches the chiral circle.

D. Four-pole solutions

TDHF solutions based on four kinks are of particular interest since we reach the level of complexity needed to describe baryon-baryon and breather-breather scattering in the GN model. These problems have already been solved recently by a different method based on an ansatz for the TDHF potential [33,34], at the expense of a substantial technical effort. It is an important cross-check of the present simpler approach to reproduce these complicated results.

From the preceding discussion, it is clear that the various four kink processes can be classified as follows: kink + kink + kink + kink, kink + kink + 2-kink, kink + kink + 2-breather, 2-kink + 2-kink, 2-kink + 2-breather, 2-breather + 2-breather, kink + 3-kink, kink + 3-breather, 4-kink, and 4-breather. Out of these, we select the following processes which are of interest for the GN model:

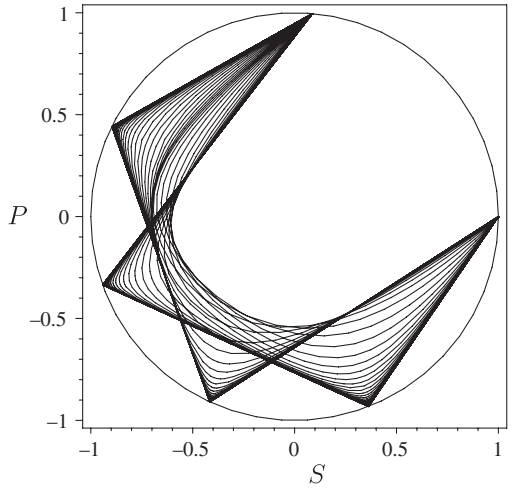

FIG. 10. (S, P) plot of the scattering process of three single, twisted kinks. The curves show the time dependence, in equal time steps. Initial and final states correspond to three-sided open polygons, all corners and end points lying on the chiral circle.

1. 2-kink+2-kink

By pairing the twist angles ($\phi_1 + \phi_2 = \phi_3 + \phi_4 = \pi$) and using a diagonal matrix ω, this particular process can be turned into scattering of two DHN baryons studied in Ref. [33]. We have checked with CA that the present closed expressions reproduce exactly the results of Ref. [33], provided one chooses the origin of the x and t axes appropriately. This calculation can now be generalized to the scattering of two twisted 2-kinks in a straightforward manner.

2. 2-breather + 2-breather

To get a real TDHF potential for breather-breather scattering, one has to pair the twist angles as in the baryon-baryon case and choose ω in the block diagonal form

$$\omega = \begin{pmatrix} \omega_{11} & \omega_{12} & 0 & 0 \\ \omega_{12}^* & \omega_{11} & 0 & 0 \\ 0 & 0 & \omega_{33} & \omega_{34} \\ 0 & 0 & \omega_{34}^* & \omega_{33} \end{pmatrix}. \tag{3.24}$$

Once again, we have checked with CA that the result agrees with the solution of breather-breather scattering in the GN model from Ref. [34]. A comparison between the complicated formulas given in Ref. [34] and the present work shows how efficient it is to take the detour via the NJL_2 model, where one can take full advantage of factorization and integrability properties of the model. Once again, the present approach allows us to repeat the calculation with twisted breathers in the NJL_2 model with modest effort, solving an even more complicated problem analytically.

3. 4-breather

An irreducible 4-kink breather of the NJL_2 model has many free parameters due to the appearance of a general, Hermitian 4×4 matrix ω. We do not study all of these complex oscillation modes here but ask the following question: How many parameters survive if we specialize the 4-breather to real Δ, i.e., a solution of the GN model? This is of some interest, since the 4-breather is the simplest TDHF solution of the GN model which cannot be reduced to the known basic building blocks of kink, baryon, and 2-breather. (There is no real 3-breather, since the chiral twists have to be paired). We have computed the TDHF potential Δ for the 4-breather at rest with CA, using $\phi_1 + \phi_2 = \phi_3 + \phi_4 = \pi$ and keeping ω general at first. We then demand that Δ is real. This puts a number of constraints on the matrix elements ω_{nm}. The most general solution can be parametrized as follows (a and e are real):

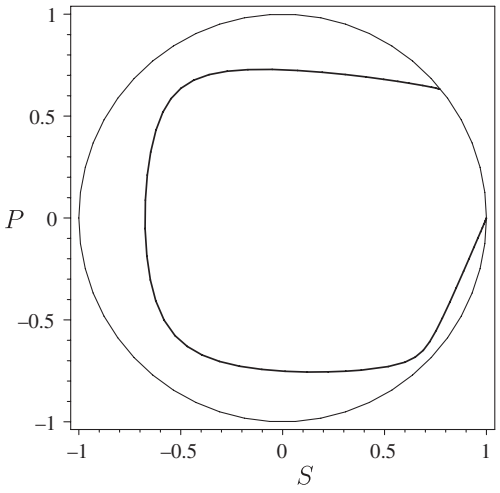

FIG. 11. (S, P) plot of a 4-kink, a bound state of four twisted kinks.

$$\omega = \begin{pmatrix} a & b & c & d \\ b^* & a & d^* & c^* \\ c^* & d & e & f \\ d^* & c & f^* & e \end{pmatrix}. \tag{3.25}$$

This leaves a lot of room for new kinds of solutions of the GN model, parametrized by the two complex parameters c, d characteristic for an irreducible 4-breather.

In Fig. 11, a 4-kink bound state at rest (parameters: $\phi_1 = 1.0$, $\phi_2 = 0.8$, $\phi_3 = 0.6$, $\phi_4 = 0.4$, $\omega_{11} = 81$, $\omega_{22} = 9$, $\omega_{33} = 1$, $\omega_{44} = 1/9$) is illustrated. Figure 12 shows the scattering of a 2-kink on a 2-kink. For animations of the complete time dependence and processes involving breathers, see the Appendix and Ref. [42] (animation_2-kink_plus_2_kink, animation_2-breather_plus_2-breather, animation_4-breather), where also an example of an irreducible 4-breather of the GN model with real $\Delta = S$ (animation_real_4-breather) can be found.

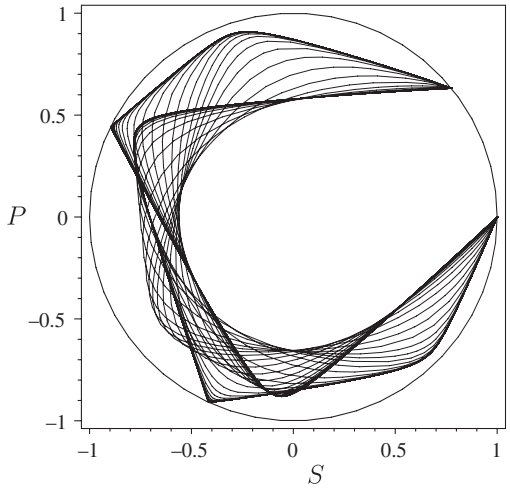

FIG. 12. (S, P) plot of the scattering process of two 2-kinks. The curves show the time dependence, in equal time steps. The initial and final states are the curves touching the chiral circle with an inner point.

IV. SUMMARY AND CONCLUSIONS

Within one year after the inception of the GN_2 model, DHN found a time-dependent multifermion solution, the breather [22]. They also realized that it is related to the kink-antikink scattering problem by analytic continuation. Somewhat surprisingly, no further progress was made on time-dependent solutions of either the GN_2 or the NJL_2 model between 1975 and 2010, to the best of our knowledge. In the present work and in Refs. [24,31], we have presented what we believe to be the full solution of the TDHF problem for both the GN_2 and NJL_2 models. Let us briefly summarize how this has been achieved.

In a first round of investigations starting in 2010, the interaction of a small number of scatterers was studied in great detail by means of an ansatz method. The scatterers involved were kinks [28], baryons [33], and breathers [34], all belonging to the GN_2 model. The ansatz consisted of multiplying the scalar potentials and spinors for the individual scatterers and then varying the coefficients of some (x, t)-dependent exponentials, until the Dirac equation was satisfied. This could be done at the expense of considerable use of computational algebra and led to the exact solutions of the problems considered. In the course of these works, many simplifying features emerged which enabled the authors to extrapolate the results to more complicated scattering processes involving N scatterers [38]. Since a general proof was lacking, these results could only be checked analytically for few body problems, up to $N = 6$. In the simplest special case, that of multikink scattering, the problem proved to be fully solvable for all N, by mapping it onto the known soliton solutions of the Sinh–Gordon equation [29].

Several developments have helped us to solve the problem in full generality in the meantime. Thus, for instance, we realized that it is advantageous to solve the NJL_2 model first and then get the GN_2 solutions in a second step by specializing to real TDHF potentials. This strategy had been overlooked for a long time and is indeed unexpected: The NJL_2 model has a more complicated Lagrangian than the GN_2 model. Moreover, its continuous chiral symmetry forbids states with localized fermion density, whereas one is just interested in such "baryonic" states in the GN_2 model. The reason why the NJL_2 model is easier to solve lies in the fact that twisted kinks are the basic constituents of all TDHF solutions, and they appear in free form only in the NJL_2 model. Nevertheless, they are also hidden constituents of GN_2 baryons and breathers, as we have shown here. As for the question of fermion density, we have shown that the same construction of the TDHF potential can be used for both models, but the self-consistency condition is different, leading to different assignments of fermion number, but with the same condensate.

A two-step procedure for solving the TDHF problem has proven most economic. In a first step, we have constructed a general family of transparent scalar-pseudoscalar Dirac potentials [31], generalizing the method used for the stationary Schrödinger equation by Kay and Moses long ago [39]. This yields closed form expressions for processes involving N twisted kinks. Depending on the parameters, they describe kinks, bound states, breathers, and scattering processes among all of these entities. In a second step reported in the present paper, we employ these transparent potentials in a TDHF calculation and prove their self-consistency. While the method is completely general, it requires diagonalization of an $N \times N$ matrix. Thus, for more than $N = 2$, it is difficult to write general analytic expressions, so the occupation fractions of the bound states are best determined numerically. We have presented examples with up to four kinks, displaying a rich spectrum of scenarios, in particular as far as breathers are concerned. If one specializes these examples to real potential, either by choosing the twist angle π or by pairing two twisted kinks to total twist 0, one recovers all the preceding results from the GN_2 model. In contrast to the earlier works, we now have the general proof of the Dirac equation and self-consistency condition as well as compact closed expressions in terms of determinants, valid for arbitrary numbers of constituent kinks. We have also learned that new kinds of breathers appear at each N, so that one cannot exhaust the dynamics of the GN_2 model via bound or scattering states of $N = 2$ objects only. The basic constituent common to all solutions is the twisted kink, which does not exist as a free entity in the GN model—it is hidden.

Characteristic for integrable models is the fact that the transmission amplitude for a fermion on a compound object factorizes in the individual kink constituents. Nevertheless, there are nontrivial backreaction effects which require fermion filling-fraction conditions for a self-consistent TDHF solution. We have shown that the factorized scattering translates into an additivity of the kink masses for all bound states and breathers. It is also the key for finding the asymptotic behavior of the solitons after the scattering has taken place. This includes in general a deformation of the soliton shape, a time delay, and (for breathers) a change in the phases of the oscillations.

Is this the end of the story? Given the fact that all static HF solutions are known, the only loophole is for the breathers. We have not yet completely ruled out that the ansatz we have used for finding transparent Dirac potentials misses some exotic breathers with an even more complicated structure. However, in view of the simplicity of the underlying Lagrangians, this seems very unlikely.

ACKNOWLEDGMENTS

G. D. acknowledges support from DOE Grants No. DE-FG02-92ER40716 and No. DE-FG02-13ER41989 and the ARC Centre of Excellence in Particle Physics at the Terascale and CSSM, School of Chemistry and Physics, University of Adelaide. M. T. thanks the DFG for financial support under Grant No. TH 842/1-1. We thank P. Dunne for assistance with the animations, which are available in the Supplemental Material.

APPENDIX: PARAMETERS USED IN THE ANIMATIONS

Here we collect the parameters used in the animations contained in the Supplemental Material to the present paper [42]. The fermion occupation fractions ν_n are not input but the result of the self-consistency condition. For kinks, they can be computed as $\nu_n = \phi_n/\pi$; therefore, they are not given below. For solutions involving breathers, the fermion occupation numbers are derived from the eigenvalues in the consistency condition (2.30), as described at the end of Sec. II B.

(i) animation_kink_plus_kink

$$\eta_1 = 2, \quad \eta_2 = 1/2 \quad \phi_1 = 1.0, \quad \phi_2 = 0.8$$
$$\omega_{11} = 3, \quad \omega_{22} = 1/3$$

(ii) animation_2-breather

$$\eta_1 = \eta_2 = 1 \qquad \phi_1 = 0.6, \qquad \phi_2 = 1.2$$
$$\chi = 1.1 \qquad \nu_1 = 0.076, \qquad \nu_2 = 0.497$$

(iii) animation _kink_plus_kink_plus_kink

$$\eta_1 = 2, \qquad \eta_2 = 1, \qquad \eta_3 = 1/2$$
$$\phi_1 = 1.0, \qquad \phi_2 = 0.8, \qquad \phi_3 = 0.6$$
$$\omega_{11} = 9, \qquad \omega_{22} = 1, \qquad \omega_{33} = 1/9$$

(iv) animation_2-kink_plus_kink

$$\eta_1 = \eta_2 = 2, \qquad \eta_3 = 1/2 \qquad \phi_1 = 1.0,$$
$$\phi_2 = 0.8, \qquad \phi_3 = 0.6 \qquad \omega_{11} = 9,$$
$$\omega_{22} = 1, \qquad \omega_{33} = 1/9$$

(v) animation_2-breather_kink_boundstate

$$\eta_1 = \eta_2 = \eta_3 = 1 \quad \phi_1 = 1.0, \quad \phi_2 = 0.8, \quad \phi_3 = 0.6$$
$$\chi = 1.4, \quad \omega_{33} = 1/81 \quad \nu_1 = 0.474, \quad \nu_2 = 0.099$$

(vi) animation_2-breather_plus_kink

$$\eta_1 = \eta_2 = 1.1, \qquad \eta_3 = 1/\eta_1$$
$$\phi_1 = 1.0, \qquad \phi_2 = 0.8, \qquad \phi_3 = 0.6$$
$$\chi = 1.4, \qquad \omega_{33} = 1/81$$
$$\nu_1 = 0.474, \qquad \nu_2 = 0.099$$

(vii) animation_3-breather

$$\eta_1 = \eta_2 = \eta_3 = 1$$
$$\phi_1 = 1.0, \qquad \phi_2 = 0.8, \qquad \phi_3 = 0.6$$
$$L = \begin{pmatrix} 2.5 & 0 & 0 \\ 2.4 & 0.5 & 0 \\ 1.65 & -0.7 & 1.0 \end{pmatrix}$$
$$\nu_1 = 0.543, \qquad \nu_2 = 0.007, \qquad \nu_3 = 0.214$$

(viii) animation_2-kink_plus_2-kink

$$\eta_1 = \eta_2 = 2, \qquad \eta_3 = \eta_4 = 1/2$$
$$\phi_1 = 1.0, \quad \phi_2 = 0.8, \quad \phi_3 = 0.6, \qquad \phi_4 = 0.4$$
$$\omega_{11} = 81, \qquad \omega_{22} = 9, \qquad \omega_{33} = 1, \qquad \omega_{44} = 1/9$$

(ix) animation_2-breather_plus_2-breather

$$\eta_1 = \eta_2 = 1.1, \qquad \eta_3 = \eta_4 = 1/\eta_1$$
$$\phi_1 = 1.0, \qquad \phi_2 = 0.8, \qquad \phi_3 = 0.6, \qquad \phi_4 = 0.4$$
$$\chi_1 = 1.1, \qquad \chi_2 = 1.2$$
$$\nu_1 = 0.357, \quad \nu_2 = 0.216, \quad \nu_3 = 0.247, \quad \nu_4 = 0.071$$

(x) animation_4-breather

$$\eta_1 = \eta_2 = \eta_3 = \eta_4 = 1$$
$$\phi_1 = 1.0, \quad \phi_2 = 0.8, \qquad \phi_3 = 0.6, \qquad \phi_4 = 0.4$$
$$L = \begin{pmatrix} 1.48 & 0 & 0 & 0 \\ 1.32 & 0.67 & 0 & 0 \\ 0 & 1.50 & 1.66 & 0 \\ 0 & 0 & 1.55 & 0.60 \end{pmatrix}$$
$$\nu_1 = 0.473, \quad \nu_2 = 0.029, \quad \nu_3 = 0.172, \quad \nu_4 = 0.217$$

(xi) animation_real_4-breather

$$\eta_1 = \eta_2 = \eta_3 = \eta_4 = 1$$
$$\phi_1 = 1.0, \quad \phi_2 = \pi - \phi_1, \quad \phi_3 = 0.6, \quad \phi_4 = \pi - \phi_3$$
$$L = \begin{pmatrix} 1.07 & 0 & 0 & 0 \\ 0.51 & 0.94 & 0 & 0 \\ 0.22 & 0.20 & 1.20 & 0 \\ 0.28 & 0.10 & 0.86 & 0.83 \end{pmatrix}$$
$$\nu_3 - \nu_1 = 0.922, \qquad \nu_4 - \nu_2 = 0.410$$

[1] D. J. Gross and A. Neveu, Phys. Rev. D **10**, 3235 (1974).
[2] Y. Nambu and G. Jona-Lasinio, Phys. Rev. **122**, 345 (1961).
[3] M. Thies, J. Phys. A **39**, 12707 (2006).
[4] G. Basar, G. V. Dunne, and M. Thies, Phys. Rev. D **79**, 105012 (2009).
[5] P. Fulde and R. A. Ferrell, Phys. Rev. **135**, A550 (1964); A. I. Larkin and Y. N. Ovchinnikov, Zh. Eksp. Teor. Fiz. **47**, 1136 (1964); [Sov. Phys. JETP **20**, 762 (1965)].
[6] R. Peierls, *The Quantum Theory of Solids* (Oxford University, New York, 1955); P. G. de Gennes, *Superconductivity of Metals and Alloys* (*Addison-Wesley*, Reading, MA, 1989).
[7] B. Horovitz, Phys. Rev. Lett. **46**, 742 (1981).
[8] S. A. Brazovskii, S. A. Gordynin, and N. N. Kirova, Pis'ma Zh. Eksp. Teor. Fiz. **31**, 486 (1980) [JETP Lett. **31**, 456 (1980)]; S. A. Brazovskii and N. N. Kirova, Pis'ma Zh. Eksp. Teor. Fiz. **33**, 6 (1981) [JETP Lett. **33**, 4 (1981)].
[9] S. Okuno and Y. Onodera, J. Phys. Soc. Jpn. **52**, 3495 (1983).
[10] K. Machida and H. Nakanishi, Phys. Rev. B **30**, 122 (1984); K. Machida and M. Fujita, Phys. Rev. B **30**, 5284 (1984).
[11] K. Machida, Physica (Amsterdam) **158**, 192 (1989).
[12] M. Kato, K. Machida, H. Nakanishi, and M. Fujita, J. Phys. Soc. Jpn. **59**, 1047 (1990).
[13] K. Rajagopal and F. Wilczek, *At the Frontier of Particle Physics; Handbook of QCD*, edited by M. Shifman and F. Wilczek (World Scientific, Singapore, 2001).
[14] R. Casalbuoni and G. Nardulli, Rev. Mod. Phys. **76**, 263 (2004).
[15] A. J. Heeger, S. Kivelson, J. R. Schrieffer, and W.-P. Su, Rev. Mod. Phys. **60**, 781 (1988).

[16] T. Mizushima, K. Machida, and M. Ichioka, Phys. Rev. Lett. **94**, 060404 (2005).
[17] M. W. Zwierlein, A. Schirotzek, C. H. Schunck, and W. Ketterle, Science **311**, 492 (2006); G. B. Partridge, W. Li, R. I. Kamar, Y. Liao, and R. G. Hulet, Science **311**, 503 (2006).
[18] S. Giorgini, L. P. Pitaevskii, and S. Stringari, Rev. Mod. Phys. **80**, 1215 (2008).
[19] A. Adams, L. D. Carr, T. Schäfer, P. Steinberg, and J. E. Thomas, New J. Phys. **14**, 115009 (2012).
[20] R. Kanamoto, L. D. Carr, and M. Ueda, Phys. Rev. Lett. **100**, 060401 (2008).
[21] C. P. Herzog, P. Kovtun, S. Sachdev, and D. T. Son, Phys. Rev. D **75**, 085020 (2007); S. Sachdev, Phys. Rev. Lett. **105**, 151602 (2010).
[22] R. F. Dashen, B. Hasslacher, and A. Neveu, Phys. Rev. D **10**, 4114 (1974); Phys. Rev. D **10**, 4130 (1974); Phys. Rev. D **12**, 2443 (1975).
[23] F. Correa, G. V. Dunne, and M. S. Plyushchay, Ann. Phys. (Amsterdam) **324**, 2522 (2009).
[24] G. V. Dunne and M. Thies, Phys. Rev. Lett. **111**, 121602 (2013).
[25] V. E. Zakharov and A. V. Mikhailov, Zh. Eksp. Teor. Fiz. **74**, 1953 (1978) [Sov. Phys. JETP **47**, 1017 (1978)]; Commun. Math. Phys. **74**, 21 (1980).
[26] K. Pohlmeyer, Commun. Math. Phys. **46**, 207 (1976).
[27] A. Neveu and N. Papanicolaou, Commun. Math. Phys. **58**, 31 (1978).
[28] A. Klotzek and M. Thies, J. Phys. A **43**, 375401 (2010).
[29] C. Fitzner and M. Thies, Phys. Rev. D **83**, 085001 (2011).
[30] A. Jevicki and K. Jin, J. High Energy Phys. 06 (**2009**) 064.
[31] G. V. Dunne and M. Thies, arXiv:1308.5801.
[32] S. -S. Shei, Phys. Rev. D **14**, 535 (1976).
[33] G. V. Dunne, C. Fitzner, and M. Thies, Phys. Rev. D **84**, 105014 (2011).
[34] C. Fitzner and M. Thies, Phys. Rev. D **87**, 025001 (2013).
[35] J. Feinberg, Ann. Phys. (Amsterdam) **309**, 166 (2004).
[36] D. A. Takahashi and M. Nitta, Phys. Rev. Lett. **110**, 131601 (2013); D. A. Takahashi, S. Tsuchiya, R. Yoshii, and M. Nitta, Phys. Lett. B **718**, 632 (2012); D. A. Takahashi and M. Nitta, arXiv:1307.3897.
[37] G. Basar and G. V. Dunne, Phys. Rev. Lett. **100**, 200404 (2008); Phys. Rev. D **78**, 065022 (2008).
[38] C. Fitzner and M. Thies, Phys. Rev. D **85**, 105015 (2012).
[39] I. Kay and H. E. Moses, J. Appl. Phys. **27**, 1503 (1956).
[40] F. Karbstein and M. Thies, Phys. Rev. D **76**, 085009 (2007).
[41] W. Brendel and M. Thies, Phys. Rev. D **81**, 085002 (2010).
[42] See Supplemental Material at http://link.aps.org/supplemental/10.1103/PhysRevD.89.025008 for animations.
[43] J. Feinberg, Phys. Lett. B **569**, 204 (2003).